Observing Internal Tides in High-Risk Regions Using Co-located Ocean Gliders and Moored ADCPs

By Rob A. Hall, Barbara Berx, and Mark E. Inall

Internal tides are an important mechanism in the cascade of kinetic energy within the ocean that ranges from large-scale surface tides to small-scale turbulent mixing. Through this cascade, internal tides contribute to the global mixing budget and drive vertical nutrient fluxes that enhance primary productivity in nutrient-limited surface waters. Although internal tides are a common phenomenon over continental shelves and slopes, as they are generated by tidal currents across sloping topography (e.g., shelf breaks, submarine ridges, canyons, and seamounts), directly observing them in these regions can be a challenge because intense commercial fishing activity increases the risk of instrument loss. Internal tide energy flux, an important diagnostic for the study of energy pathways in the ocean, requires repeated full-depth measurements of both potential density and horizontal current velocity over at least a tidal cycle (several weeks to resolve the internal spring-neap cycle). Typically, these measurements are made using an acoustic Doppler current profiler (ADCP) and a string of conductivity-temperature loggers on a mooring line, or a moored profiler with a CTD and a current meter. These full-depth moorings are vulnerable to being “fished-out” by demersal and pelagic trawling.

Recently, autonomous ocean gliders have been used to map internal tide propagation, either from the amplitude and phase of vertical isopycnal displacement over a wide area (Rainville et al., 2013; Boettger et al., 2015; Hall et al., in press) or combined with glider-mounted ADCPs to directly calculate energy flux (Johnston et al., 2013, 2015). Here, we propose a complementary approach to determine internal tide energy flux at key fixed locations that uses current velocity measurements collected with a low-frequency ADCP, moored on or near the seabed, and density measurements collected using a glider holding station as a “virtual mooring” over the ADCP. High temporal resolution is crucial. Nash et al. (2005) suggest a minimum of four evenly distributed independent profiles are required per tidal cycle. Gliders can safely dive with vertical velocities up to 20 cm s^{-1}, so this is easily achievable for semidiurnal (~12-hour period) and diurnal (~24-hour) internal tides down to 1,000 m. The depth-limiting factor is the ADCP’s range: a single near-bottom 75 kHz ADCP can sample 80%–90% of a 700 m water column, but it is less likely to be fished-out by pelagic trawling than a full-depth mooring. Risk from demersal trawling can be minimized by mounting the ADCP in a trawl-resistant frame. Being relatively small, the glider is unlikely to be fished-out, and risk of surface collision can be reduced by real-time evasive action in response to approaching vessels, guided by the maritime Automatic Identification System (AIS).

This new approach was tested over the continental slope north of Scotland during August 2014. An iRobot 1KA Seaglider (SG510; Eriksen et al., 2001) was deployed from MPV *Jura* for 10 days to hold station over a short, twin ADCP (75 kHz upward-looking and 300 kHz downward-looking at ~635 m; 85% depth coverage) mooring on the 700 m isobath (Figure 1). An antenna fault caused the glider’s GPS positions and satellite telemetry to rapidly degrade, but it still managed to hold station within 4 km of the mooring for two 12.42-hour periods (near a barotropic spring tide and a barotropic neap tide). An auxiliary Argos tag on the glider’s antenna provided surface location.

During these two periods, semidiurnal velocity perturbations and density anomalies were extracted from the ADCP and glider time series, respectively, using M_2 tidal period (12.42-hour) harmonic analyses on depth levels. Eighty percent of the total isopycnal displacement variance in the main pycnocline can be attributed to the M_2 internal tide. Internal tide energy flux was calculated from the covariance of baroclinic velocity and pressure perturbations following Nash et al.

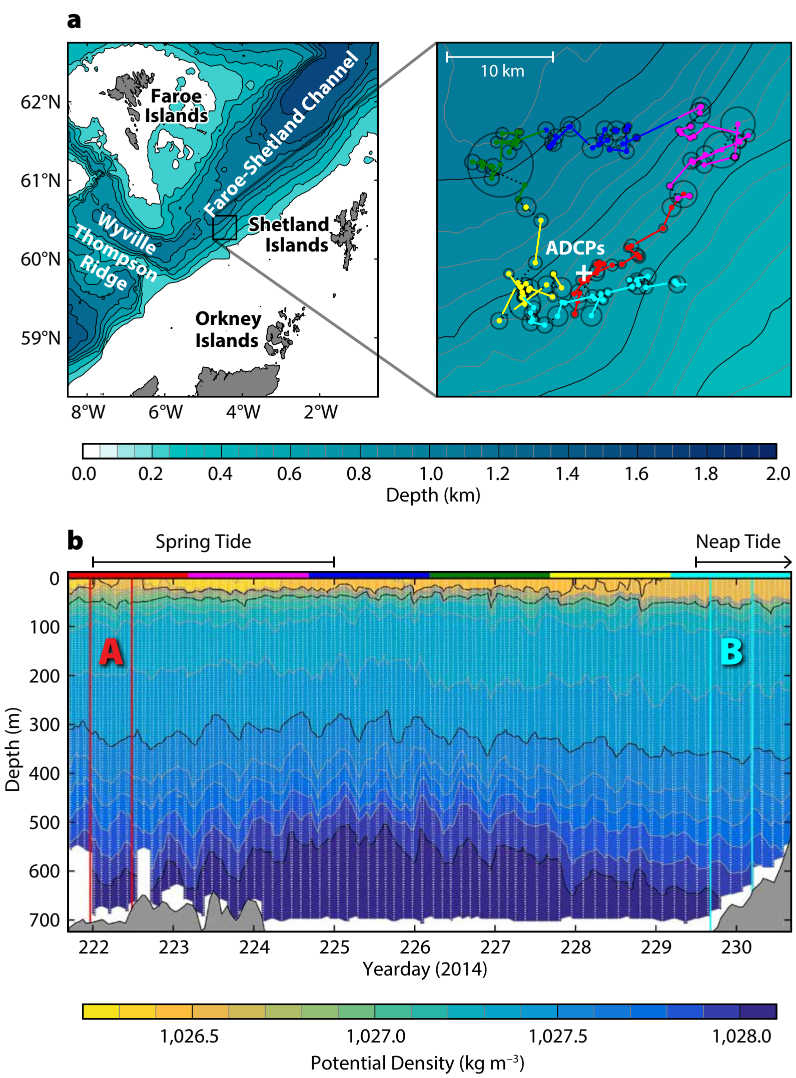

FIGURE 1. (a) Path of the glider over the continental slope. Samples are separated into six consecutive 36-hour windows: colored dots are surface locations (gray circles indicate Argos location error), colored lines are subsurface trajectories, and black dotted lines are surface drift. (b) Potential density time series. White dotted lines trace glider paths and show the temporal resolution. A and B are two periods when the glider and ADCP data sets were co-located.

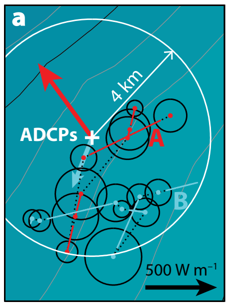

FIGURE 2. (a) Path of the glider during two non-consecutive 12.42-hour periods, A (red) and B (cyan), when it was within 4 km of the ADCP mooring. The thick arrows indicate depth-integrated semidiurnal internal tide energy flux during the two periods. (b) Across-slope and (d) along-slope baroclinic velocity (color), overlaid with vertical isopycnal displacement (black lines), during period A. Profiles of (c) across-slope and (e) along-slope energy flux for the two periods: solid lines indicate both glider and ADCP data coverage, and dashed lines indicate that one of the data sets required interpolation/extrapolation. Positive velocities and fluxes are upslope and along-slope to the northeast.

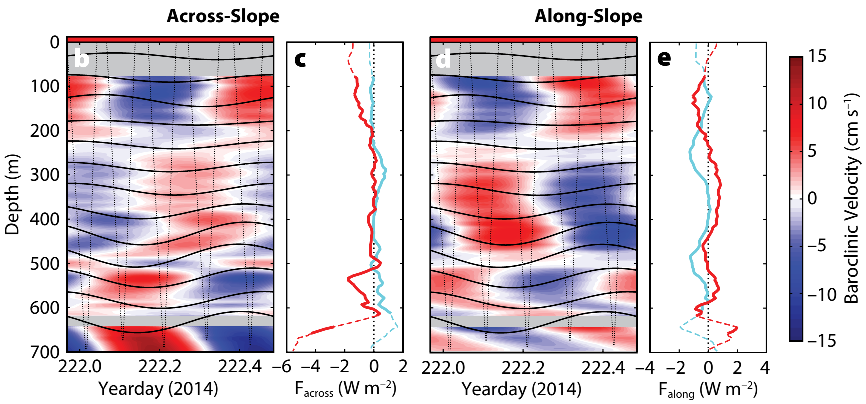

(2005). The glider's 2.8-hour average dive time yielded 4.4 independent near-bottom samples each semidiurnal tidal cycle. By processing the descending and ascending profiles separately, the number of mid-depth samples was doubled. Although not ideal, 4 km is considered reasonable co-location for the purpose of observing the semidiurnal internal tide; theoretical mode-1 horizontal wavelength is ~80 km at the location of the mooring (calculated from measured buoyancy frequency).

Near spring tide (period A), semidiurnal internal tide energy flux was downslope in the bottom 200 m (up to 5.5 W m^{-2}) and in the upper 200 m (up to 1.5 W m^{-2}) of the water column, but near zero between these layers. Along-slope energy flux was positive (northeastward) and negative (southwestward) in alternating layers and almost cancels under depth integration. Overall, depth-integrated energy flux was 620 W m^{-1} and directed downslope (Figure 2). Seven days later, near neap tide (period B), across-slope energy flux was smaller (<1.5 W m^{-2}) and primarily upslope, while along-slope energy flux was southwestward in almost all layers and up to 2 W m^{-2}. Depth-integrated energy flux (360 W m^{-1}) was around half that at spring tide and directed south-southwest. This direction is in agreement with observations made at a nearby location (15 km southwest) during September 2005 (Hall et al., 2011), again close to a neap tide. During this previous study, depth-integrated energy flux was 208 W m^{-1}, smaller than both estimates here, but buoyancy frequency through the main pycnocline at 600 m was notably higher. Deep stratification in the Faroe-Shetland Channel is highly variable due to changes in water mass circulation and mesoscale variability. This will affect local internal tide generation, remote generation (e.g., at the Wyville Thompson Ridge and over the Faroe slope; Hall et al., 2011), and local reflection of remotely generated internal tides (Hall et al., 2013). Varying influence of these processes could result in the observed temporally variable internal tide field.

During this work, navigation and communication difficulties limited the co-location of the glider and ADCP data sets, as well as the glider's endurance. However, experience from other missions suggests that a fully functional glider operating as a virtual mooring is able to stay within 2.5 km of its target location, and can do so for several months, depending on its sensor payload. Moving into deeper water, the current generations of both Seagliders and Slocum gliders can operate to 1,000 m, and three-hour dives to this depth are easily achievable. New generation gliders will dive deeper and for longer, but aliasing issues will arise; three-hour dives are at the half-Nyquist limit of semidiurnal resolution (four near-surface and four near-bottom samples per tidal cycle). A greater limitation is the ~600 m range of current generation 75 kHz ADCPs. The new generation of 55 kHz ADCPs will increase range to ~1,000 m and so will be ideal for combining with a glider virtual mooring. In addition, glider-derived dive-average current velocity (Eriksen et al., 2001) could be used to help separate the barotropic and baroclinic components in the absence of full-depth data coverage by the ADCP.

This new approach, combining a glider virtual mooring with a moored ADCP in regions of intense commercial fishing activity, has the potential to yield multiple-month time series of internal tide energetics. This will allow resolution of multiple tidal constituents, the internal spring-neap cycle, and evolution of the internal tide field in response to seasonally changing stratification and mesoscale eddy activity.

REFERENCES

Eriksen, C.C., T.J. Osse, R.D. Light, T. Wen, T.W. Lehman, P.J. Sabin, J.W. Ballard, and A.M. Chiodi. 2001. Seaglider: A long-range autonomous underwater vehicle for oceanographic research. *IEEE Journal of Oceanic Engineering* 26:424–436, https://doi.org/10.1109/48.972073.

Boettger, D., R. Robertson, and L. Rainville. 2015. Characterizing the semidiurnal internal tide off Tasmania using glider data. *Journal of Geophysical Research* 120:3,730–3,746, https://doi.org/10.1002/2015JC010711.

Hall, R.A., T. Aslam, and V.A.I. Huvenne. In press. Partly standing internal tides in a dendritic submarine canyon observed by an ocean glider. *Deep Sea Research Part I*, https://doi.org/10.1016/j.dsr.2017.05.015.

Hall, R.A., J.M. Huthnance, and R.G. Williams. 2011. Internal tides, nonlinear internal wave trains, and mixing in the Faroe-Shetland Channel. *Journal of Geophysical Research* 116, C03008, https://doi.org/10.1029/2010JC006213.

Hall, R.A., J.M. Huthnance, and R.G. Williams. 2013. Internal wave reflection on shelf slopes with depth-varying stratification. *Journal of Physical Oceanography* 43:248–258, https://doi.org/10.1175/JPO-D-11-0192.1.

Johnston, T.M.S., D.L. Rudnick, M.H. Alford, A. Pickering, and H.L. Simmons. 2013. Internal tidal energy fluxes in the South China Sea from density and velocity measurements by gliders. *Journal of Geophysical Research* 118:3,939–3,949, https://doi.org/10.1002/jgrc.20311.

Johnston, T.M.S., D.L. Rudnick, and S.M. Kelly. 2015. Standing internal tides in the Tasman Sea observed by gliders. *Journal of Physical Oceanography* 45:2,715–2,737, https://doi.org/10.1175/JPO-D-15-0038.1.

Nash, J.D., M.H. Alford, and E. Kunze. 2005. Estimating internal wave energy fluxes in the ocean. *Journal of Atmospheric and Oceanic Technology* 22:1,551–1,570, https://doi.org/10.1175/JTECH1784.1.

Rainville, L., C.M. Lee, D.L. Rudnick, and K.-C. Yang. 2013. Propagation of internal tides generated near Luzon Strait: Observations from autonomous gliders. *Journal of Geophysical Research* 118:4,125–4,138, https://doi.org/10.1002/jgrc.20293.

ACKNOWLEDGMENTS

SG510 is owned and maintained by the UEA Marine Support Facility. The glider and ADCP mooring were deployed as part of the UK Natural Environment Research Council FASTNEt project (NE/I030224/1) and the Marine Scotland Science Offshore Monitoring Programme. Assistance with glider piloting was provided by the UEA Glider Science group and the data processed using the UEA Seaglider Toolbox (https://bitbucket.org/bastienqueste/uea-seaglider-toolbox).

AUTHORS

Rob A. Hall (robert.hall@uea.ac.uk) is Lecturer, Centre for Ocean and Atmospheric Sciences, University of East Anglia, Norwich, UK. **Barbara Berx** is Physical Oceanographer, Marine Scotland Science, Aberdeen, UK. **Mark E. Inall** is Professor, Scottish Association for Marine Science, Oban, UK, and Honorary Professor, School of Geoscience, University of Edinburgh, UK.

ARTICLE CITATION

Hall, R.A., B. Berx, and M.E. Inall. 2017. Observing internal tides in high-risk regions using co-located ocean gliders and moored ADCPs. *Oceanography* 30(2):51–52, https://doi.org/10.5670/oceanog.2017.220.